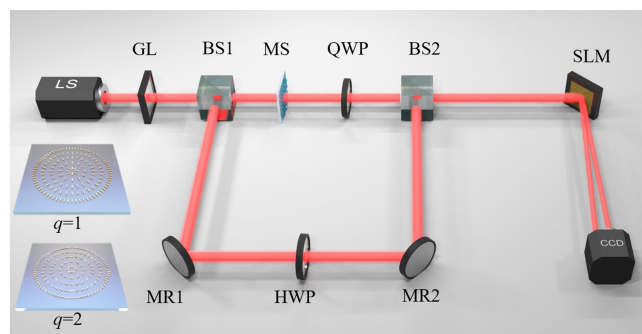


# Effectively Identifying the Topological Charge and Polarization Order of Arbitrary Singular Light Beams Based on Orthogonal Polarization Separating

Volume 11, Number 6, December 2019

Yanliang He  
Huapeng Ye  
Junmin Liu  
Zhiqiang Xie  
Peipei Wang  
Bo Yang  
Xinxing Zhou  
Yanxia Gao  
Shuqing Chen  
Ying Li  
Dianyuan Fan



---

DOI: 10.1109/JPHOT.2019.2944968

# Effectively Identifying the Topological Charge and Polarization Order of Arbitrary Singular Light Beams Based on Orthogonal Polarization Separating

Yanliang He<sup>1</sup>, Huapeng Ye<sup>2</sup>, Junmin Liu<sup>3</sup>, Zhiqiang Xie<sup>1</sup>,  
Peipei Wang<sup>1</sup>, Bo Yang<sup>1</sup>, Xinxing Zhou<sup>1</sup>, Yanxia Gao<sup>1</sup>,  
Shuqing Chen<sup>1</sup>, Ying Li<sup>1</sup>, and Dianyuan Fan<sup>1</sup>

<sup>1</sup>International Collaborative Laboratory of 2D Materials for Optoelectronics Science and Technology, and Engineering Technology Research Center for 2D Material Information Function Devices and Systems of Guangdong Province, Institute of Microscale Optoelectronics, Shenzhen University, Shenzhen 518060, China

<sup>2</sup>Guangdong Provincial Key Laboratory of Optical Information Materials and Technology & Institute of Electronic Paper Displays, South China Academy of Advanced Optoelectronics, South China Normal University, Guangzhou 510006, China

<sup>3</sup>College of New Materials and New Energies, Shenzhen Technology University, Shenzhen 518118, China

<sup>4</sup>Synergetic Innovation Center for Quantum Effects and Applications, School of Physics and Electronics, Hunan Normal University, Changsha 410081, China

DOI:10.1109/JPHOT.2019.2944968

This work is licensed under a Creative Commons Attribution 4.0 License. For more information, see <https://creativecommons.org/licenses/by/4.0/>

Manuscript received April 8, 2019; revised September 21, 2019; accepted September 28, 2019. Date of publication October 1, 2019; date of current version October 31, 2019. This work was supported in part by the National Natural Science Foundation of China under Grants 61805149, 61575127, 61490713, and 61571188, in part by the Guangdong Natural Science Foundation under Grant 2016A030310065, in part by the Program of Fundamental Research of Shenzhen Science and Technology Plan under Grants JCYJ20180507182035270 and GJHZ20180928160407303, in part by the Science and Technology Planning Project of Guangdong Province under Grant 2016B050501005, in part by the Science and Technology Project of Shenzhen under Grant ZDSYS201707271014468, in part by the International Collaborative Laboratory of 2D Materials for Optoelectronics Science and Technology under Grant 2DMOST2018003, and in part by the Educational Commission of Guangdong Province under Grant 2016KCXTD006. (Yanliang He and Huapeng Ye contributed equally to this work.) Corresponding author: Ying Li (email: queenly@szu.edu.cn).

**Abstract:** Singular beams with spatially variant field distributions have various fantastic applications. However, one of the significant challenges that hinder the wide application of singular beams is how to effectively identify the topological charge and the polarization order of arbitrary singular beams. We found that when a light beam with arbitrary polarization state illuminates a polarization-sensitive blazed-grating, the horizontal and vertical component can be separated from the incident beam. Based on this phenomenon, an effective method is proposed to probe the integral topological charge and polarization order of arbitrary singular beams. With this detection method, the vortex beam, cylindrical vector beam and cylindrical vector vortex beam with different topological charges and polarization orders have been experimentally identified. This effective detection method can be widely used to measure the topological charge and polarization order of arbitrary singular beams.

**Index Terms:** Singular beam, orthogonal polarization separating, helical phase.

## 1. Introduction

Structured light beams have attracted intensive attention due to their spatially variant field distributions. As two kinds of typically structured light beams, vortex beam (VB) carrying orbital angular momentum (OAM) and cylindrical vector beam (CVB) possessing phase singularity and polarization singularity respectively, have been extensively studied [1]–[10]. Both of them have an annular intensity distribution with a dark spot arising from their central singularity [1], [6]. Integral VB and CVB have been also demonstrated to be an eigenstate of OAM and vector mode [11], [12]. Due to their unique optical properties, optical vortices and CVBs have been widely applied in various applications ranging from optical communications [12]–[17], optical manipulation [18]–[24], to quantum information processing [25]–[27] and optical imaging [28], [29].

Generally, light beams with phase singularity and polarization singularity simultaneously provide more freedom for beam manipulation [30], [31]. These beams are also called cylindrical vector vortex beams (CVVBs) and have attracted extensive attentions in optical manipulation [32]–[35]. Plenty of approaches have been proposed to generate singular beams [36]–[46]. However, apart from creating high-quality singular beams, it is also crucial to effectively identify their topological charge and polarization order. As the spatial field distributions of singular beams are different from each other, the method of estimating their topological charge and polarization order should also be different. Usually, the interferometry is used to determine the topological charge of VB, while the polarizer is widely used to detect the polarization order of CVB and CVVB. However, none of existing detecting methods can be commonly used to effectively determine the topological charge and polarization order of arbitrary singular beams.

In this article, we propose and demonstrate an effective method for arbitrary singular beams detection based on orthogonal polarization separation. A polarization-sensitive blazed-grating which is obtained with the phase-type spatial light modulator (SLM) and is only responsive to the horizontally polarized component, is employed to separate the horizontally and vertically polarized components of the incident beam. In the experiment, the Gaussian beam from the laser with the working wavelength of 1550 nm is split into two sub-beams. One of the sub-beams is used to produce the desired singular beam, while the other is polarized to 45 degrees for interfering. After the orthogonal circularly polarized components of the CVB or CVVB are transformed into orthogonal linearly polarized components, the coaxial transformed singular beam and Gaussian beam are projected to the SLM for polarization separation and mutual interference. Finally, by determining the topological charges of each components, the topological charges and polarization orders of the optical vortices (the topological charges are 1, 2, 3, 4), CVBs (the polarization orders are 2, -2, 4, -4) and CVVBs (the topological charges and polarization orders are (1, 2), (2, 2), (3, 2), (4, 2)) are successfully identified.

## 2. Theoretical Analysis

Singular beams including VB, CVB, and CVVB can be simply written as

$$e^{i\theta} \begin{bmatrix} 1 \\ 1 \end{bmatrix} = e^{i\theta} \begin{bmatrix} 1 \\ 0 \end{bmatrix} + e^{i\theta} \begin{bmatrix} 0 \\ 1 \end{bmatrix}, \quad (1)$$

$$\begin{bmatrix} \cos(m\theta + \phi) \\ \sin(m\theta + \phi) \end{bmatrix} = \frac{1}{2} e^{i\phi} e^{im\theta} \begin{bmatrix} 1 \\ -i \end{bmatrix} + \frac{1}{2} e^{-i\phi} e^{-im\theta} \begin{bmatrix} 1 \\ i \end{bmatrix}, \quad (2)$$

$$e^{i\theta} \begin{bmatrix} \cos(m\theta + \phi) \\ \sin(m\theta + \phi) \end{bmatrix} = \frac{1}{2} e^{i\phi} e^{i(l+m)\theta} \begin{bmatrix} 1 \\ -i \end{bmatrix} + \frac{1}{2} e^{-i\phi} e^{i(l-m)\theta} \begin{bmatrix} 1 \\ i \end{bmatrix}, \quad (3)$$

where  $l$  is the topological charge,  $\theta$  is the azimuthal angle,  $\phi$  is the initial phase and  $m$  is the polarization order.

After passing through the quarter-wave plate (QWP) whose fast axis is rotated to 45 degrees, the orthogonal circularly polarized components of CVB and CVVB are transformed into orthogonal

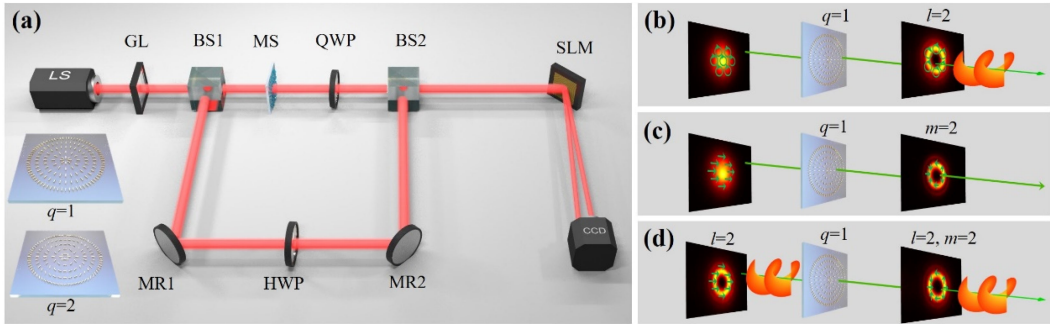


Fig. 1. (a) Experimental setup to measure the topological charge and polarization order of arbitrary singular beams; LS: light source, GL: Glan laser polarizer, BS: beam splitter, MR: mirror, MS: metasurface, QWP: quarter-wave plate, HWP: half-wave plate, SLM: spatial light modulator, CCD: charge-coupled devices; the inserts are the theoretical optical axis distributions of the MS with  $q = 1$  and  $q = 2$ . (b-d) Schematic illustration of the mechanism to generate VB, CVB and CVVB with MS respectively, where the green arrows represent the predicted polarization states.

linearly polarized components, namely

$$\frac{1}{2} e^{i\phi} e^{im\theta} \begin{bmatrix} 1 & -i \\ -i & 1 \end{bmatrix} \begin{bmatrix} 1 \\ -i \end{bmatrix} + \frac{1}{2} e^{-i\phi} e^{-im\theta} \begin{bmatrix} 1 & -i \\ -i & 1 \end{bmatrix} \begin{bmatrix} 1 \\ i \end{bmatrix} = e^{i\phi} e^{im\theta} \begin{bmatrix} 0 \\ 1 \end{bmatrix} + e^{-i\phi} e^{-im\theta} \begin{bmatrix} 1 \\ 0 \end{bmatrix}, \quad (4)$$

$$\frac{1}{2} e^{i\phi} e^{i(l+m)\theta} \begin{bmatrix} 1 & -i \\ -i & 1 \end{bmatrix} \begin{bmatrix} 1 \\ -i \end{bmatrix} + \frac{1}{2} e^{-i\phi} e^{i(l-m)\theta} \begin{bmatrix} 1 & -i \\ -i & 1 \end{bmatrix} \begin{bmatrix} 1 \\ i \end{bmatrix} = e^{i\phi} e^{i(l+m)\theta} \begin{bmatrix} 0 \\ 1 \end{bmatrix} + e^{-i\phi} e^{i(l-m)\theta} \begin{bmatrix} 1 \\ 0 \end{bmatrix}. \quad (5)$$

In order to detect the topological charge of the horizontal and vertical components of the singular beam, the Gaussian beam, which is used to interfere with the singular beam, must contain both horizontally polarized and vertically polarized components. Moreover, the Gaussian beam should be polarized along 45 degrees and coaxial with the transformed singular beam. The phase-type SLM is polarization sensitive, which can only modulate the horizontally polarized component of the incident beam [47]. Based on this, we upload a blaze-grating on the SLM to diffract the horizontally polarized beam, and the vertically polarized beam is only reflected. As we properly design the period of the blaze-grating, the reflected vertically polarized beam and the diffracted horizontally polarized beam will be separated. After modulated by the polarization-sensitive blazed-grating, the horizontal and vertical components of the Gaussian beam and the transformed singular beam are separated and interfere with each other, respectively. The normal blazed-grating can be expressed as

$$2d \sin \alpha \cos(\alpha - \beta) = n\lambda, n = 1, 2, 3 \dots, \quad (6)$$

where  $d$  is the grating constant,  $\alpha$  is the blazed angle,  $\beta$  is the angle of incidence, and  $\lambda$  is the wavelength of incident beam.  $n$  can take any positive integer.

After the topological charges of horizontally polarized component ( $h$ ) and vertically polarized component ( $v$ ) are obtained, the topological charge ( $l$ ) or polarization order ( $m$ ) of arbitrary singular beams can be calculated by

$$l = \frac{v + h}{2}, m = \frac{v - h}{2}. \quad (7)$$

### 3. Experimental Setup and Results

The experimental setup of determining the topological charge and the polarization order of arbitrary singular beams is shown in Fig. 1(a). A laser beam with the working wavelength of 1550 nm is generated from a continuous wave laser and then filtered by a Glan laser polarizer (GL). It is split into two sub-beams by the beam splitter (BS). One of the sub-beams is further modulated by the

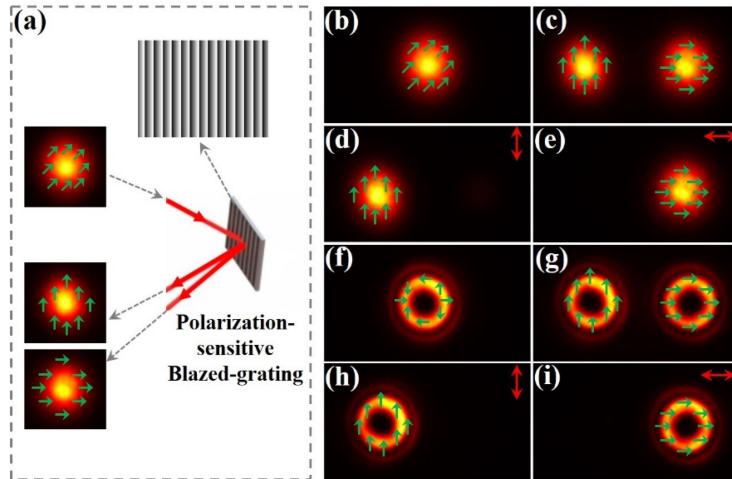


Fig. 2. (a) Schematic illustration of separating the linearly polarized Gaussian beam with polarization-sensitive blazed-grating. (b) and (f) are the intensity distributions of incident light of Gaussian beam and CVB. (c) and (g) are the intensity distributions of emergent light. (d–e) and (h–i) are the intensity distributions with a polarizer placed behind the polarization-sensitive blazed-grating, where the red bidirectional arrows represent the polarization orientation of polarizer. The green arrows represent the predicted polarization states.

metasurface (MS) and results in VB, CVB or CVVB. Meanwhile, the other sub-beam is modulated by the half-wave plate (HWP) and polarized along 45 degrees for interfering with the singular beam along the other light path. According to our previous study [44], VB or CVB can be created by a single MS. Hence, we can easily obtain CVVB by cascading two MSs and adjusting the polarization state of the incident light. Here, the MS is fabricated by etching space-variant nanograting on a fused silica substrate with a femtosecond laser and thus has a space-variant birefringence. Desired polarization distributions can be realized by adjusting the local orientation and geometrical parameter of the grooves.

The mechanism of creating arbitrary singular beams with MS is depicted in Figs. 1(b–d). In order to illustrate the properties of the MS, the optical axis distributions of the MS with  $q = 1$  and  $q = 2$  are also plotted in the inserts of Fig. 1(a). Here,  $q$  is a constant indicating the spatial rotation ratio of the optical axis. According to the previous introduction, the orthogonal circularly polarized components of CVB and CVVB should be transformed into orthogonal linearly polarized components before it reaches the polarization-sensitive blazed-grating which is realized by loading the desired phase pattern on the phase-only SLM (PLUTO-TELCO-013).

Fig. 2(a) schematically illustrates the principle of how to separate the linearly polarized Gaussian beam with polarization-sensitive blazed-grating. As shown in Fig. 2(a), when a Gaussian beam polarizing along 45 degrees is projected to the SLM with a blazed-grating period of  $160 \mu\text{m}$  and efficiency up to 81%, the horizontal linearly polarized component is diffracted with an angle much bigger than the incident angle. To achieve the best performance of the SLM, the incident angle is controlled as less than 6 degrees, the reflective angle of the vertical linearly polarized component is equal to the incidence, and the blazed angle of the blazed-grating is about 20 degrees. This phenomenon is experimentally verified as shown in Figs. 2(b–i), where orthogonal linearly polarized beams are successfully separated. A linearly polarized Gaussian beam with the polarization state of 45 degrees and a CVB with polarization order of 2 are depicted, respectively. From Figs. 2(c) and 2(g), we can see that the coaxial orthogonal linearly polarized components are separated into two parts, whereas other diffraction orders are almost negligible. Moreover, a polarizer which is polarized along 0 degree or 90 degrees is placed behind the SLM to indicate the polarization status of the beam, as shown in Figs. 2(d–e) and 2(h–i).

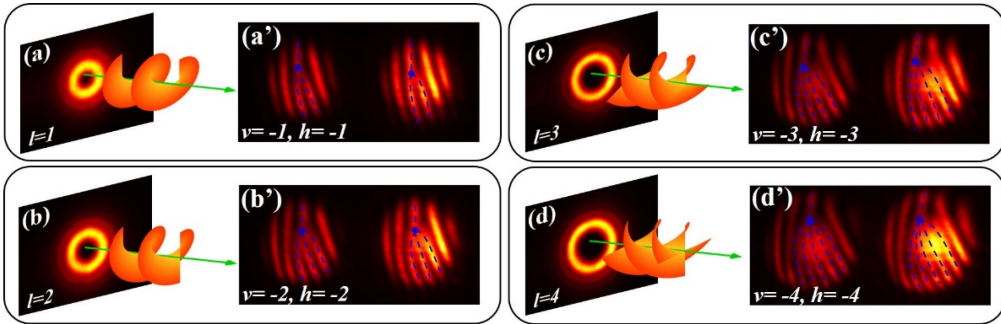


Fig. 3. (a–d) Intensity distributions of the optical vortices with different topological charges (1, 2, 3 and 4), (a'–d') interference fringes of the planar wave with two separated linearly polarized components respectively, where the blue dashed represents the dislocated condition.

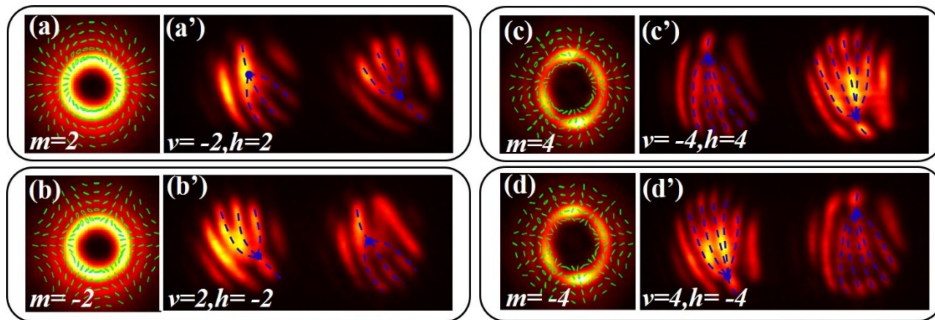


Fig. 4. (a–d) Intensity distributions of the CVBs with different polarization orders (2,  $-2$ , 4, and  $-4$ ), (a'–d') interference fringes of the planar wave with two separated linearly polarized components respectively, where the green ellipses represent the polarization states, and the blue dashed represents the dislocated condition.

Based on the polarization-sensitive blazed-grating, we have further measured the topological charge or polarization order of VB, CVB, and CVVB. The linearly polarized Gaussian beam is transformed to left-handed circularly polarized Gaussian beam by a QWP. After passing through the MS, a right-handed circularly polarized VB with a positive topological charge is produced ( $l = 1, 2, 3, 4$  are chosen). The intensity distributions of the produced optical vortices are shown in Figs. 3(a–d). After that, the circularly polarized optical vortices whose polarization states are 45 degrees by another QWP behind the MS. The resulting beam combines with the reference Gaussian beam which is also polarized to 45 degrees and then comes to the SLM. The interference fringes are shown in Figs. 3(a'–d'). It is evident that the number of dislocated interference fringes is one more than the topological charge [48]. Generally speaking, when the topological charge is a positive integer, the direction of the fork fringes is oblique upward. Conversely, the direction of the fork fringes is oblique downward. The practical topological charges of the optical vortices can be calculated with Eq. (7). It can be also found that the estimated topological charge is opposite to the theoretical value, which is caused by single reflection after passing through the SLM. Finally, the calculated topological charges of the optical vortices are given as 1, 2, 3 and 4.

According to Eqs. (2–3), CVB and CVVB can be split into two orthogonal circularly polarized optical vortices. Theoretically, the topological charges of these two components are different. When a linearly polarized Gaussian beam passes the MS, CVBs ( $m = 2, -2, 4, -4$  are chosen) can be obtained. The intensity distributions of the produced CVBs are shown in Figs. 4(a–d). After that, the orthogonal circularly polarized component is further modulated by a QWP and turns into the

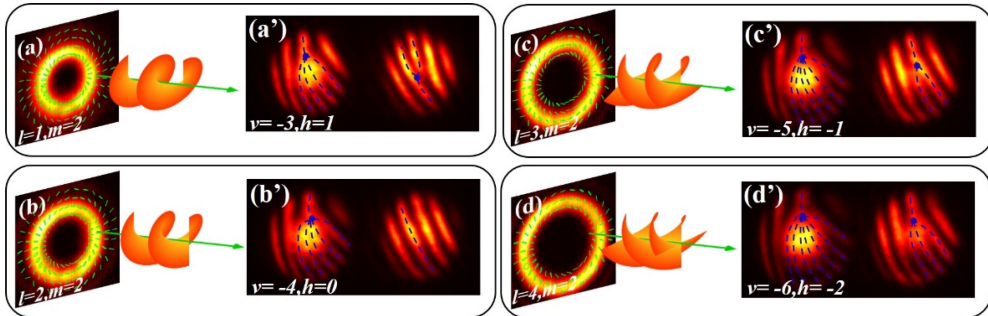


Fig. 5. (a–d) Intensity distributions of the CVVBs with different topological charges and polarization orders ((1, 2), (2, 2), (3, 2) and (4, 2)), (a'–d') interference fringes of the planar wave with two separated linearly polarized components respectively, where the green ellipses represent the polarization states, and the blue dashed represents the dislocated condition.

orthogonal linearly polarized component. After interfering with the reference Gaussian beam, the interference fringes are detected and depicted in Figs. 4(a–d'). Due to the single reflection of SLM, the topological charges of each components are reversed. The practical polarization orders of CVBs can be calculated with Eq. (7). Finally, the calculated polarization orders of CVBs are given as 2, -2, 4 and -4. In order to effectively demonstrate that the polarization state of CVB is desirable, we have measured the polarization states of CVB with Stokes polarization reconstructed method [49]. Firstly, the exact parameter values of any state from the Stokes parameters are extracted. Then, according to the relationship of the Stokes parameters and polarization, the polarization states of CVBs are achieved, as shown in Figs. 4(a–d).

Furthermore, the proposed system is used to measure the topological charge and polarization order of CVVB. In order to generate CVVB, circularly polarized VB is firstly obtained by modulating a circularly polarized Gaussian beam with a MS. It is transformed into linearly polarized VB by a QWP behind the MS. This linearly polarized beam is further modulated by another MS and finally leads to CVVB. Their intensity and polarization distributions are shown in Figs. 5(a–d), while the topological charges of each component of CVVBs are identified and plotted in Figs. 5(a'–d'). After the topological charges of each component are estimated, the topological charges and polarization orders of CVVBs can be calculated with Eq. (7). The calculated topological charges and polarization orders of CVVBs are given as (1, 2), (2, 2), (3, 2) and (4, 2).

As a proof of concept, we have used a reference Gaussian beam to create interference fringes. In the practical application, we can apply the diffraction methods to measure the topological charges of the two optical vortices after they are separated with the polarization-sensitive blazed-grating. By diffracting the two optical vortices through the cylindrical lens [50], triangle aperture [51] or some other particular designed elements [52], the topological charges of the two decomposed optical vortices can also be obtained from the diffraction patterns. In addition, the proposed scheme is mainly focused on the standard singular beams. For the complex singular beam with complicated mode components, it is also worth studying in depth. Some researchers have proposed utilizing the designed polarization-insensitive MS to measure multichannel vortices [45]. In the future, we can try to design a polarization-sensitive MS to measure multichannel vortices with orthogonally polarization states simultaneously, and realizing the detection of arbitrary complex singular beams. Besides, we can achieve more flexible and versatile applications by integrating metalens, etc. [53], [54] into the MS.

#### 4. Conclusions

In summary, we have experimentally demonstrated an effective detection method based on orthogonal polarization separation for measuring the topological charge and polarization order of

arbitrary singular beams. In our proposal, the singular beam is firstly transformed by a QWP and then recombines with the reference Gaussian beam. When the coaxial singular beam and reference Gaussian beam passes through the sensitive-polarized blazed-grating, the horizontally polarized and vertically polarized components of the singular beam and Gaussian beam are successfully separated and then interfering with each other. The optical vortices (the topological charges are 1, 2, 3, 4), CVBs (the polarization orders are 2, -2, 4, -4) and CVVBs (the topological charges and polarization orders are (1, 2), (2, 2), (3, 2), (4, 2)) with different topological charges and polarization orders are successfully detected with this method. This detection method provides a new avenue to effectively measure the topological charge and polarization order of arbitrary singular beams.

## References

- [1] L. Allen, M. W. Beijersbergen, R. J. C. Spreeuw, and J. P. Woerdman, "Orbital angular momentum of light and the transformation of Laguerre-Gaussian laser modes," *Phys. Rev. A*, vol. 45, no. 11, pp. 8185–8189, Jun. 1992.
- [2] A. M. Yao and M. J. Padgett, "Orbital angular momentum: origins, behavior and applications," *Adv. Opt. Photon.*, vol. 3, no. 2, pp. 161–204, May 2011.
- [3] H. Ye *et al.*, "Intrinsically shaping the focal behavior with multi-ring bessel-gaussian beam," *Appl. Phys. Lett.*, vol. 111, no. 3, pp. 1–890, Jul. 2017.
- [4] Y. Yang, X. Zhu, J. Zeng, X. Lu, C. Zhao, and Y. Cai, "Anomalous bessel vortex beam: Modulating orbital angular momentum with propagation," *Nanophotonics*, vol. 7, no. 3, pp. 677–682, Nov. 2017.
- [5] S. Fu and C. Gao, "Influences of atmospheric turbulence effects on the orbital angular momentum spectra of vortex beams," *Photon. Res.*, vol. 4, no. 5, pp. B1–B4, Oct. 2016.
- [6] Q. Zhan, "Cylindrical vector beams: from mathematical concepts to applications," *Adv. Opt. Photon.*, vol. 1, no. 1, pp. 1–57, Jan. 2009.
- [7] K. S. Youngworth and T. G. Brown, "Focusing of high numerical aperture cylindrical-vector beams," *Opt. Exp.*, vol. 7, no. 2, pp. 77–87, Jul. 2000.
- [8] X-L. Wang, J. Ding, J. Qin, J. Chen, Y. Fan, and H-T. Wang, "Configurable three-dimensional optical cage generated from cylindrical vector beams," *Opt. Commun.*, vol. 282, no. 17, pp. 3421–3425, May 2009.
- [9] Y. Yuan, T. Lei, S. Gao, X. Weng, L. Du, and X-C. Yuan, "The orbital angular momentum spreading for cylindrical vector beams in turbulent atmosphere," *IEEE Photon. J.*, vol. 9, no. 2, Apr. 2017, Art. no. 6100610.
- [10] W. Cheng, J. W. Haus, and Q. Zhan, "Propagation of vector vortex beams through a turbulent atmosphere," *Opt. Exp.*, vol. 17, no. 20, pp. 17829–17836, Sep. 2009.
- [11] S. J. van Enk, and G. Nienhuis, "Eigenfunction description of laser beams and orbital angular momentum of light," *Opt. Commun.*, vol. 94, no. 1-3, pp. 147–158, Nov. 1992.
- [12] G. Milione *et al.*, "4 × 20 Gbit/s mode division multiplexing over free space using vector modes and a q-plate mode (de) multiplexer," *Opt. Lett.*, vol. 40, no. 9, pp. 1980–1983, May 2015.
- [13] J. Liu *et al.*, "Direct fiber vector eigenmode multiplexing transmission seeded by integrated optical vortex emitters," *Light Sci. Appl.*, vol. 7, no. 3, Mar. 2018, Art. no. 17148.
- [14] G. Milione, T. A. Nguyen, J. Leach, D. A. Nolan, and R. R. Alfano, "Using the nonseparability of vector beams to encode information for optical communication," *Opt. Lett.*, vol. 40, no. 21, pp. 4887–4890, Nov. 2015.
- [15] J. Wang *et al.*, "Terabit free-space data transmission employing orbital angular momentum multiplexing," *Nature Photon.*, vol. 6, no. 7, pp. 488–496, Jun. 2012.
- [16] G. Gibson *et al.*, "Free-space information transfer using light beams carrying orbital angular momentum," *Opt. Exp.*, vol. 12, no. 22, pp. 5448–5456, Oct. 2004.
- [17] X. Zhang *et al.*, "Coherent separation detection for orbital angular momentum multiplexing in free-space optical communications," *IEEE Photon. J.*, vol. 9, no. 3, Jun. 2017, Art. no. 7903811.
- [18] S. Yan and B. Yao, "Radiation forces of a highly focused radially polarized beam on spherical particles," *Phys. Rev. A*, vol. 76, no. 5, Nov. 2007, Art. no. 053836.
- [19] T. A. Nieminen, N. R. Heckenberg, and H. R. Dunlop, "Forces in optical tweezers with radially and azimuthally polarized trapping beams," *Opt. Lett.*, vol. 33, no. 2, pp. 122–124, Jan. 2008.
- [20] H. He, M. E. J. Fries, N. R. Heckenberg, and H. R. Dunlop, "Direct observation of transfer of angular momentum to absorptive particles from a laser beam with a phase singularity," *Phys. Rev. Lett.*, vol. 75, no. 5, pp. 826–829, Jul. 1995.
- [21] J. Ng, Z. Lin, and C-T. Chan, "Theory of optical trapping by an optical vortex beam," *Phys. Rev. Lett.*, vol. 104, no. 10, Mar. 2010, Art. no. 103601.
- [22] Y. Ke, Y. Liu, Y. He, J. Zhou, H. Luo, and S. Wen, "Realization of spin-dependent splitting with arbitrary intensity patterns based on all-dielectric metasurfaces," *Appl. Phys. Lett.*, vol. 107, no. 4, Jul. 2015, Art. no. 041107.
- [23] X. Ling *et al.*, "Recent advances in the spin Hall effect of light," *Rep. Prog. Phys.*, vol. 80, no. 6, Mar. 2017, Art. no. 066401.
- [24] Y. Li *et al.*, "Observation of photonic spin Hall effect with phase singularity at dielectric metasurfaces," *Opt. Exp.*, vol. 23, no. 2, pp. 1767–1774, Jan. 2015.
- [25] A. Mair, A. Vaziri, G. Weihs, and A. Zeilinger, "Entanglement of the orbital angular momentum states of photons," *Nature*, vol. 412, no. 6844, pp. 313–316, Jul. 2011.
- [26] A. H. Ibrahim, F. S. Roux, M. McLaren, T. Konrad, and A. Forbes, "Orbital-angular-momentum entanglement in turbulence," *Phys. Rev. A*, vol. 88, no. 1, Jul. 2013, Art. no. 012312.

- [27] J. Leach *et al.*, "Quantum correlations in optical angle-orbital angular momentum variables," *Science*, vol. 329, no. 5992, pp. 662–665, Aug. 2010.
- [28] D. S. Simon and A. V. Sergienko, "Two-photon spiral imaging with correlated orbital angular momentum states," *Phys. Rev. A*, vol. 85, no. 4, Apr. 2012, Art. no. 043825.
- [29] D. P. Biss, K. S. Youngworth, and T. G. Brown, "Dark-field imaging with cylindrical-vector beams," *Appl. Opt.*, vol. 45, no. 3, pp. 470–479, Jan. 2006.
- [30] Z. Zhao, J. Wang, S. Li, and A. E. Willner, "Metamaterials-based broadband generation of orbital angular momentum carrying vector beams," *Opt. Lett.*, vol. 38, no. 6, pp. 932–934, Mar. 2013.
- [31] C-W. Qiu *et al.*, "Engineering light-matter interaction for emerging optical manipulation applications," *Nanophotonics*, vol. 3, no. 3, pp. 181–201, Dec. 2014.
- [32] E. Otte, C. Alpmann, and C. Denz, "Polarization singularity explosions in tailored light fields," *Laser Photon. Rev.*, vol. 12, no. 6, May 2018, Art. no. 1700200.
- [33] A. D'Erico *et al.*, "Topological features of vector vortex beams perturbed with uniformly polarized light," *Sci. Rep.*, vol. 7, Jan. 2017, Art. no. 40195.
- [34] C. E. R. Souza, J. A. O. Huguenin, and A. Z. Khouri, "Topological phase structure of vector vortex beams," *J. Opt. Soc. America A*, vol. 31, no. 5, pp. 1007–1012, May 2014.
- [35] A. Niv, G. Biener, V. Kleiner, and E. Hasman, "Manipulation of the Pancharatnam phase in vectorial vortices," *Opt. Exp.*, vol. 14, no. 10, pp. 4208–4220, May 2006.
- [36] B. Huang, Q. Yi, L. Yang, C. Zhao, and S. Wen, "Controlled higher-order transverse mode conversion from a fiber laser by polarization manipulation," *J. Opt.*, vol. 20, no. 2, Jan. 2018, Art. no. 024016.
- [37] R. Chen *et al.*, "High efficiency all-fiber cylindrical vector beam laser using a long-period fiber grating," *Opt. Lett.*, vol. 43, no. 4, pp. 755–758, Feb. 2018.
- [38] D. Naidoo *et al.*, "Controlled generation of higher-order Poincaré sphere beams from a laser," *Nature Photon.*, vol. 10, no. 5, pp. 327–332, Mar. 2016.
- [39] F. Yue *et al.*, "Multichannel polarization-controllable superpositions of orbital angular momentum states," *Adv. Mater.*, vol. 29, no. 15, Feb. 2017, Art. no. 1603838.
- [40] M. Q. Mahmood *et al.*, "Visible-frequency metasurface for structuring and spatially multiplexing optical vortices," *Adv. Mater.*, vol. 28, no. 13, pp. 2533–2539, Feb. 2016.
- [41] L. Li *et al.*, "Generation of optical vortex array along arbitrary curvilinear arrangement," *Opt. Exp.*, vol. 26, no. 8, pp. 9798–9812, Apr. 2018.
- [42] R. Wang *et al.*, "Electrically driven generation of arbitrary vector vortex beams on the hybrid-order Poincaré sphere," *Opt. Lett.*, vol. 43, no. 15, pp. 3570–3573, Aug. 2018.
- [43] Y. He *et al.*, "Order-controllable cylindrical vector vortex beam generation by using spatial light modulator and cascaded metasurfaces," *IEEE Photon. J.*, vol. 9, no. 5, Oct. 2017, Art. no. 6101710.
- [44] Y. He *et al.*, "Switchable phase and polarization singular beams generation using dielectric metasurfaces," *Sci. Rep.*, vol. 7, no. 1, pp. 6814–6824, Jul. 2017.
- [45] K. Ou *et al.*, "High efficiency focusing vortex generation and detection with polarization-insensitive dielectric metasurfaces," *Nanoscale*, vol. 10, no. 40, pp. 19154–19161, Sep. 2018.
- [46] G. Li, B. P. Clarke, J-K. So, K. F. MacDonald, and N. I. Zheludev, "Holographic free-electron light source," *Nature Commun.*, vol. 7, Dec. 2016, Art. no. 13705.
- [47] Y. Zhao and J. Wang, "High-base vector beam encoding/decoding for visible-light communications," *Opt. Lett.*, vol. 40, no. 21, pp. 4843–4846, Nov. 2015.
- [48] I. D. Maleev and G. A. Swartzlander, "Composite optical vortices," *J. Opt. Soc. America B*, vol. 20, no. 6, pp. 1169–1176, Jun. 2003.
- [49] Y. Liu, X. Ling, X. Yi, X. Zhou, H. Luo, and S. Wen, "Realization of polarization evolution on higher-order Poincaré sphere with metasurface," *Appl. Phys. Lett.*, vol. 104, no. 19, May 2014, Art. no. 191110.
- [50] J. Zhou, W. Zhang, and L. Chen, "Experimental detection of high-order or fractional orbital angular momentum of light based on a robust mode converter," *Appl. Phys. Lett.*, vol. 108, no. 11, Mar. 2016, Art. no. 111108.
- [51] Y. Liu, H. Tao, J. Pu, and B. Lu, "Detecting the topological charge of vortex beams using an annular triangle aperture," *Opt. Laser Technol.*, vol. 43, no. 7, pp. 1233–1236, Oct. 2011.
- [52] X. Chen *et al.*, "Orbital angular momentum modes identification of optical vortices using binaural circular aperture," *J. Opt.*, vol. 21, no. 6, May 2019, Art. no. 065603.
- [53] H. Yang *et al.*, "Broadband polarization resolving based on dielectric metalenses in the near-infrared," *Opt. Exp.*, vol. 26, no. 5, pp. 5632–5643, Mar. 2018.
- [54] H. Yang *et al.*, "Polarization-independent metalens constructed of antennas without rotational invariance," *Opt. Lett.*, vol. 42, no. 19, pp. 3996–3999, Oct. 2017.